Bi-composite sandwich moldings: Processing, mechanical performance and bioactive behavior

R. A. SOUSA[1,2,3*], A. L. OLIVEIRA[2], R. L. REIS[1,2], A. M. CUNHA[1], M. J. BEVIS[3]
[1]*Department of Polymer Engineering, University of Minho, 4800-058 Guimarães, Portugal*
[2]*3B's Research Group – Biomaterials, Biodegradables and Biomimetics, University of Minho, Campus de Gualtar, 4710-057 Braga, Portugal*
[3]*Wolfson Centre for Materials Processing, Brunel University, Uxbridge, Middlesex UB8 3PH, UK*
E-mail: rasousa@dep.uminho.pt

Two composite systems composed of high-density polyethylene (HDPE) filled with hydroxyapatite (HA) and carbon fiber (C fiber) were compounded in a co-rotating twin screw extruder and subsequently molded in a two component injection molding machine in order to produce test bars with a sandwich-like morphology. These moldings are based on a HDPE/HA composite outer layer and a HDPE/C fiber composite core. The mechanical performance of the obtained specimens was assessed by tensile and impact testing. The fracture surfaces were observed by scanning electron microscopy (SEM) and optical reflectance microscopy was used to characterize the morphology within the moldings. In order to study the bioactivity of the molded specimens, the samples were immersed for different periods of time up to 30 days in a simulated-body fluid (SBF) with an ion composition similar to human blood plasma. After each immersion period, the surfaces of the specimens were characterized by SEM. The chemical composition and the structure of the deposited films were studied by electron dispersive spectroscopy (EDS) and thin-film X-ray diffraction (TF-XRD). The evolution of the elemental concentrations in the SBF solution was determined by induced coupled plasma emission (ICP) spectroscopy. Bi-composite moldings featuring a sandwich-like morphology were successfully produced. These moldings present a high stiffness as a result of the C fiber reinforcement present in the molding core. Furthermore, as a result of the HA loading, the sandwich moldings exhibit a clear *in vitro* bioactive behavior under simulated physiological conditions, which indicates that an *in vivo* bone-bonding behavior can be expected for these materials.

1. Introduction

The bone analog concept was introduced by Bonfield [1] in 1983, when proposing the composites of high-density polyethylene (HDPE) filled with hydroxyapatite (HA) as bone replacement materials. These composites mimic the bone composition, as they comprise a synthetic polymer (HDPE) and a stiff filler (HA), in clear analogy with the organic (collagen) and the inorganic (hydroxyapatite) phases present in bone.

The unique properties of bone result from the combination of a specific structure and the complex arrangement of the collagen and the HA crystals at different microstructural levels [2–8]. This fact makes the replication of the bone specific properties in a man-designed composite very challenging task. This can hardly be achieved through a research strategy that is exclusively based on the reinforcement of a polymeric matrix by HA particles.

In load bearing applications, the success of an implant depends on two main items: (i) the ability of the implant material to bond to the bone tissue (referred as bone bonding ability); and (ii) the adequate loading of the healing bone during the service time of the implant. Concerning the first requirement, the bonding capability is favored when a biological active apatite layer is present at its surface [9]. A material is said to be bioactive when it is capable of inducing the nucleation and the growth of such apatite layer under physiological conditions. Regarding the second requirement, the loading of any healing tissue is dependent on the stiffness of the implant that ideally should match that of the bone. This ideal situation is particularly difficult to achieve in a synthetic designed composite, since bone, in terms of mechanical performance, is a very stiff material, exhibiting values of tensile modulus, in the longitudinal direction, in the range of 7–25 GPa [10–11].

Therefore, an implant material for hard tissue replacement should combine a clear bioactive character

* Author to whom all correspondence should be addressed.

with a bone matching mechanical performance. The incorporation of HA particles in the HDPE matrix assures the desired bioactive behavior of the composite, and simultaneously provides some stiffening of the ductile phase. Nevertheless, this two-fold objective has limitations. The bone bonding capability is favored by high filler amounts (typically around 50–70 wt %), which confers a brittle behavior to these materials. Furthermore, the efficiency of the HA particles as mechanical reinforcement of the polymer matrix is reduced, due to its inherent particulate nature and low degree of interfacial interaction with the HDPE phase [12]. The application of pre-implantation treatments that induce the formation of an apatite layer at the surface of the implant material [13] can be a possible route to circumvent such problems. This method should ensure the desired bone-bonding character of the implant, by means of a biomimetic surface coating, without necessarily employing bioactive reinforcements. Such an approach enables the use of alternative and highly efficient reinforcement systems that are more adequate for tailoring the implant mechanical performance. Another possibility is the selective reinforcement of the implant, limiting the use of bioactive filler particles to the surface, where a clear bioactive behavior is desired, while high stiffness reinforcements (like carbon or aramid fiber) are used at the core of the implant in order to meet the levels of stiffness desired for the intended field of application.

This work reports the development of moldings exhibiting a sandwich-like morphology that comprise a bioactive outside composite layer and a stiff composite core. This composite is based on a HDPE matrix charged with HA particles in the outside layer and reinforced with carbon fiber (C fiber) in the inside part. C fiber were selected as reinforcement due to the respective mechanical properties and their inert biomedical character. The HDPE/HA surface layer was selected to ensure specific surface properties, while the HDPE/C fiber core is intended to guarantee the mechanical performance of the so-called bi-composite within the desired range of stiffness. This strategy is expected to enable the development of HDPE-based load bearing implants with complex geometry, controlled chemical properties and high mechanical performance. This research methodology complements the parallel research attempts followed by the authors in order to extend the mechanical performance of HDPE [14] and HDPE/HA composite systems [12, 15, 16]. These works aimed to induce a high anisotropic character to HDPE and HDPE/HA composites through the control of the structure development in injection molding [12, 14, 15]; the optimization of the HA reinforcing effect by means of the enhancement of particulate dispersion [12] and the use of C fiber as high stiffness reinforcements [16]. This paper addresses the processing by mono-sandwich injection molding of the bi-composite material, with emphasis on the study of the morphological development during injection molding and its correlation with the mechanical performance exhibited by the produced samples. Furthermore, in order to confer the bone-bonding ability of the sandwich moldings, the respective *in vitro* bioactive behavior was investigated. Structural, chemical and morphological analysis of the apatite layers formed were performed and related with the chemical evolution of the solution along the time of immersion.

2. Materials and methods

2.1. Materials

The studied material was a HDPE, grade GM9255 F, supplied by Elenac GmbH (Germany), with a melt flow index (MFI) of 0.56 g/600 s (49 N).

The HA powder used was a sintered grade, from Plasma Biotal Ltd (United Kingdom), with an average particle size of 10.1 μm and a specific surface area of 0.38 m^2/g. A neoalkoxy zirconate, designated as NZ 12, supplied by Kenrich Petrochemicals (USA), was used additionally for the HDPE/HA composite.

Composites of HDPE with C fiber were produced using chopped C fiber with a 7 μm diameter and a cut length of 6 mm, type HTA 5U41, from Tenax Fibers, GmbH & Co. (Germany).

2.2. TSE compounding

Composites of HDPE with 50% by weight (wt) HA (MFI of 0.22 g/600 s (49 N)) were produced in a Leistritz AG-LSM 36/25D modular co-rotating twin screw extruder using a screw speed of 100 rpm (output rate of 3.4 kg/h) and a temperature profile (from feeding to die zone) of 150/155/160/170/175/180/190/180 °C. The extrudate was cooled in air and subsequently pelletized by a rotating knife. The composite formulation included 0.5 wt % NZ12 (relative to the HA fraction). In a previous study [12], the use of this specific zirconate additive was found to improve considerably the HA particle dispersion in the HDPE matrix.

Short fiber reinforced composites of HDPE with 25 wt % C fiber were also compounded in the TSE equipment, using a screw speed of 40 rpm (output rate of 5.0 kg/h) and a temperature profile of 160/180/190/195/200/205/210/200 °C. Two separate polymer and fiber feeding ports were used, in order to reduce, as much as possible, the fiber breakage during melting and conveying of the polymer. A volumetric feeder and a gravimetric dosing device assured, during extrusion, the feeding of the polymer and the C fiber, respectively. The cooling of the extrudate was performed in air and then hand-chopped in 5 cm long segments to be used in the subsequent injection molding stage.

2.3. Injection molding

Two specimen geometries were molded: (i) tensile test bars with a rectangular cross of $4 \times 10\,mm^2$ and (ii) impact test bars with a rectangular cross-section of $6 \times 12.7\,mm^2$. Both specimens were produced in a two-component injection molding K-85 Ferromatik-Milacron machine using the mono-sandwich technique [17]. The injection molding conditions used are presented in Table I. In this table, the plasticizing stroke ratio refers to the ratio between the stroke of the horizontal unit (that contains the core material) and the stroke of the vertical unit (that contains the skin material).

TABLE I Processing conditions used for sandwich injection molding of HDPE/HA and HDPE/C fiber composites

	Tensile	Impact
Injection pressure* (MPa)	7.5	7.5
Holding pressure – stage 1* (MPa)	6.5	10.0
Holding pressure – stage 2* (MPa)	9.0	12.0
Injection time (s)	0.4	5.0
Holding pressure time – stage 1 (s)	15.0	10.0
Holding pressure time – stage 2 (s)	25.0	50.0
Cooling time (s)	30.0	10.0
Cycle time (s)	50.4	75.0
mold temperature (°C)	50	50
Melt temperature – barrel H† (°C)	250	200
Melt temperature – barrel V† (°C)	250	250
Plasticizing stroke ratio (mm/mm)	0.63	0.64

* Hydraulic pressure in the machine.
† H, horizontal unit (core material); V: vertical unit (skin material).

2.4. Mechanical characterization

The tensile tests were performed on an Instron 4505 universal testing machine fitted with an Instron 2630 resistive extensometer with 10 mm of gage length. The tensile test bars were tested in order to determine the tangent modulus (E_t), the ultimate tensile strength (UTS) and the strain at break (ε_f). The tests were performed in a controlled environment (23 °C and 55% RH) with a crosshead speed of 5 mm/min (8.3×10^{-5} m/s) until 1.5% strain, to determine accurately the modulus, and then increased to 50 mm/min (8.3×10^{-4} m/s) until rupture.

Impact tests were conducted in an instrumented falling weight impact machine Rosand Type 5. The tests were performed at a test speed of 3 m/s, according to a flexural scheme, using a support with 32 mm span and a 25 kg anvil. For each test, the force at peak (F_p), the peak energy (U_p) and the failure energy (U_f) were determined.

2.5. Optical microscopy

Samples for optical microscopy were obtained by cutting several zones of the test bars along the flow path and subsequent embedding in an epoxy resin. For the tensile specimens, sections were taken from the gage length at 60, 90 and 120 mm from the gate point. For the impact test bars, sections were obtained at distances of 0, 20, 40, 60, 80 and 100 mm from the gate point. After the curing of the resin, the immersed zones were carefully polished in order to obtain a smooth surface for subsequent observation by stereo light microscopy in a Nikon SMZ 10 microscope. The average thickness of the HDPE/HA composite outer layer in the moldings was quantified by measuring its thickness at 6 points along the cross section perimeter.

2.6. Bioactivity testing

The bioactive character of the moldings was studied using 10 mm length specimens (dimensions of $10 \times 10 \times 4\,\text{mm}^3$) obtained from the gauge length of the tensile test bars. Two types of samples were used: (i) unpolished (as molded); and (ii) polished (after surface grinding of the specimens using a 500 mesh SiC abrasive paper). The grinding of the molding surface was intended to increase both the roughness and the HA concentration at the surface of the specimens. This polishing could be the final technological step in the production of the bi-composite implants. The samples were immersed in a simulated body fluid (SBF), with an ion concentration nearly equal to the human blood plasma (see Table II) at physiological conditions of temperature and pH of 37 °C and 7.4, respectively, for periods of time of 3, 7, 15 and 30 days. At the end of each immersion period the samples were immediately cleaned with distilled water and dried in controled conditions (23 °C, 55% RH) for 48 h. The pH of the solutions was measured for each immersion period after removal of the samples. Being bioinert, HDPE was used as a negative control during the bioactivity tests.

2.7. Scanning electron microscopy

Scanning electron microscopy (SEM) was conducted on a Leica Cambridge instrument for morphological characterization of selected fracture surfaces and of the films formed during the bioactivity tests. All the surfaces were mounted on a copper stub and coated with C prior examination.

2.8. Energy dispersive spectroscopy

The chemical composition of the films formed during the bioactivity testing was quantified, in terms of the Ca/P and (Ca + Na + Mg + K)/P ratios, by energy dispersive spectroscopy (EDS) on a Roentec instrument.

2.9. Thin-film X-ray diffraction (TF-XRD)

The structure of the films was studied after each immersion period by thin-film X-ray diffraction (TF-XRD). Cu Kα radiation with a wavelength of 1.54 nm was used to obtain X-ray diffraction spectra in a Rigaku diffractometer. The diffraction data was acquired at a rate of 0.02° 2θ/s and over a Bragg angle range of $5° < 2\theta < 55°$.

2.10. Induced coupled plasma emission spectroscopy

The evolution of the elemental concentrations of the Ca and P ions in the SBF solution with time was determined

TABLE II Ion concentration of the simulated body fluid (SBF) and the human blood plasma

	Na^+	K^+	Ca^{2+}	Mg^{2+}	Cl^-	HCO_3^-	HPO_4^{2-}	SO_4^{2-}
SBF	142.0	5.0	2.5	1.5	147.8	4.2	1.0	0.5
Human plasma	142.0	5.0	2.5	1.5	103.0	27.0	1.0	0.5

by induced coupled plasma emission (ICP) spectroscopy in a Jovin Yvon 70 plus equipment.

3. Results and discussion

3.1. Mechanical properties and morphology of the bi-composite moldings

Fig. 1 presents the typical tensile test curves of the sandwich bi-composite moldings and the composites of HDPE/C fiber (included here as reference) together with the respective values of tangent modulus (E_t) and ultimate tensile strength (UTS). The real HA and C fiber weight contents for the sandwich bi-composite moldings, as determined by pyrolysis of the polymer matrix (4 h at 450 °C) of the HDPE/HA and the HDPE/C fiber composites, were 47% and 21% respectively, while for the HDPE/C fiber moldings the fiber content was 20 wt. %. It is evident that the stiffness and strength of the bi-composite moldings (E_t of 5.6 GPa) is considerably lower than that presented by the HDPE/C fiber composites (E_t of 8.5 GPa). This behavior is expected considering two factors: (i) the inferior fiber content present in the sandwich molding, since the C fiber are essentially restricted to the molding core; (ii) and the presence of HA particles with a limited reinforcing capability in a relatively thick skin region. A previous study by Reis *et al*. [15] on the tensile behavior of injection molded HDPE filled with HA, reported values of stiffness of about 4 GPa for a HA weight content of 50%. The low strength exhibited by the sandwich moldings is attributed to the existence of this heavily filled skin. For an identical HA weight content, Reis *et al*. [15] reported values of UTS in the 20–40 MPa range.

The evolution of the average outer layer thickness along the flow path of the tensile bars is presented in Fig. 2 together with the respective cross-section micrographs. The sandwich morphology is clearly asymmetrical, as a result of the lateral position of the gate point that unbalances the morphological development of the skin and gives rise to a thicker HDPE/HA layer in the wall opposite to the gate point. Nevertheless, this morphological asymmetry attenuates along the flow path (please compare the micrographs at 60 and 120 mm). The interpenetration of the two composite materials is also evident, as a result of the similar rheological behavior of the skin and core materials. An even distribution of the core material is favored by high viscosity ratios (core material viscosity/skin material viscosity) [18]. In spite of the uneven distribution of the core material, the penetration of the core composite was not enough, in any of the bars produced, to reach the surface of the molding, which could compromise the desired bioactivity of the implant material. The increase of the HDPE/HA composite layer thickness observed in Fig. 2 results from the advancement of the progressively cooler melt front during the filling stage. An investigation of the co-injection molding process [19] showed that the evolution of the outer skin thickness in sandwich moldings was mainly dependent on the injection speed, the injection temperature and the volume of core material. Constant core dimensions are favored by low core temperatures and high core volumes. Any further study of the processing and properties of sandwich moldings of HDPE/HA and HDPE/C fiber should consider the optimization of the processing parameters, in order to minimize the morphological asymmetry and outer layer thickness variation along the flow path.

Fig. 3 presents the SEM photographs of the fracture surface of the bi-composite moldings after tensile testing. The sandwich like morphology of the moldings is evident in Fig. 3(a). The HDPE/HA surface layer is considerably thicker along the cross-section thickness due to higher cooling rates near the molding edges. The detailed view of the transition region between the surface layer and the molding core, presented in Fig. 3(b), evidences the distinct plastic deformation behavior of the two composite materials. The HDPE/HA reinforced surface layer exhibits a pronounced brittle character, while the HDPE/C fiber core shows considerable signs of plastic deformation. The HDPE/C fiber core, in evidence in Fig. 3(c), exhibits two regions with two distinct fiber orientation patterns: (i) a shell zone, in which fibers are predominantly parallel to the main direction of flow (MDF) and (ii) a central zone where the fibers are mostly

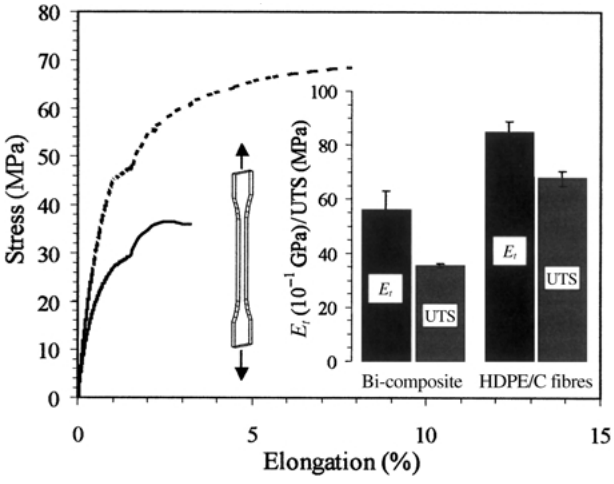

Figure 1 Typical tensile test curves for the sandwich bi-composite (solid line) and the HDPE/C fiber composite (dashed line) moldings together with the respective averaged values of E_t and UTS (please note the scale difference).

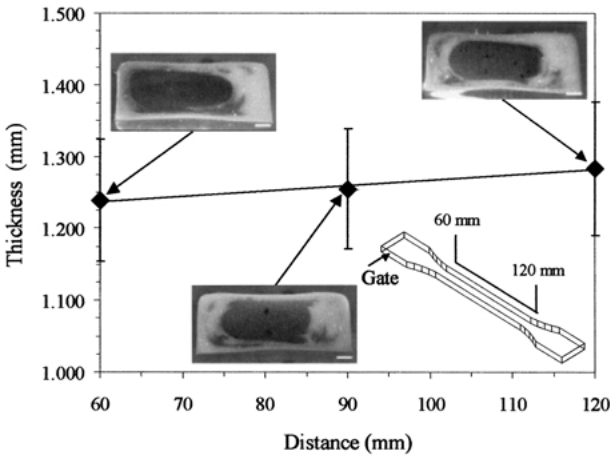

Figure 2 Variation of the average outer layer thickness along the flow path for the tensile test bars together with the cross section micrographs at 60, 90 and 120 mm from the gate point (scale bar is 1 mm).

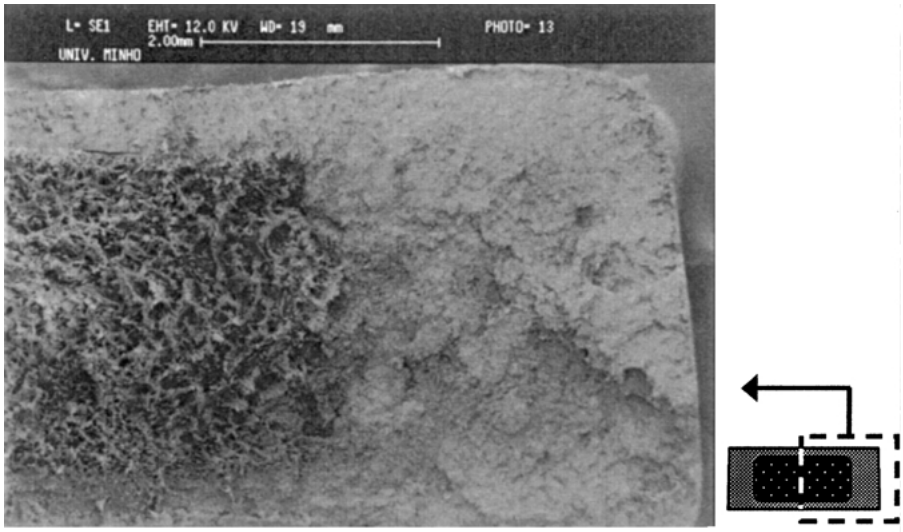

(a)

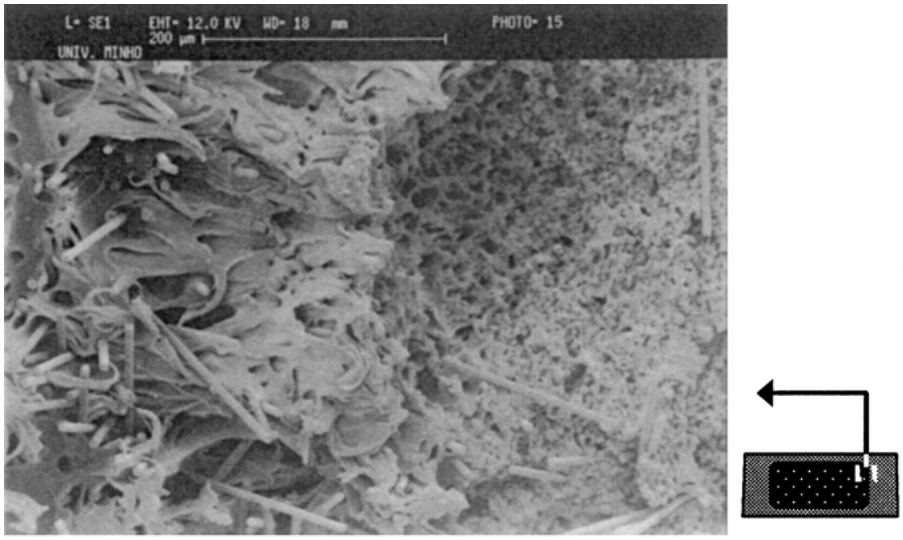

(b)

(c)

Figure 3 Scanning electron microscope (SEM) photographs of the fracture surface of the bi-composite moldings after tensile testing: (a) general view, (b) detailed view of the transition region between the HDPE/HA outer layer and the HDPE/C fiber core and (c) detailed view of the HDPE/C fiber core region.

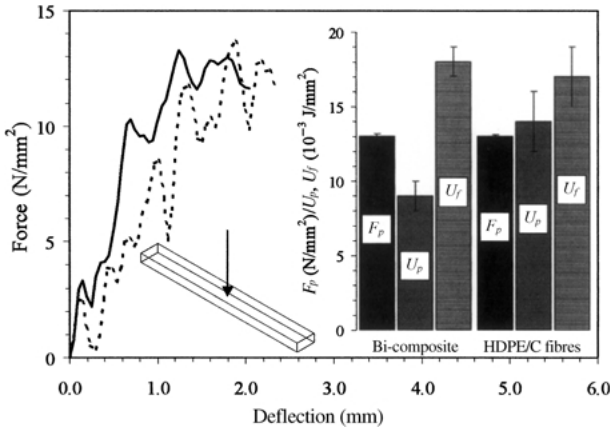

Figure 4 Typical impact test curves of the sandwich bi-composite (solid line) and the HDPE/C fiber composite (dashed line) moldings together with the respective averaged values of F_p, U_p and U_b normalized by the corresponding cross section.

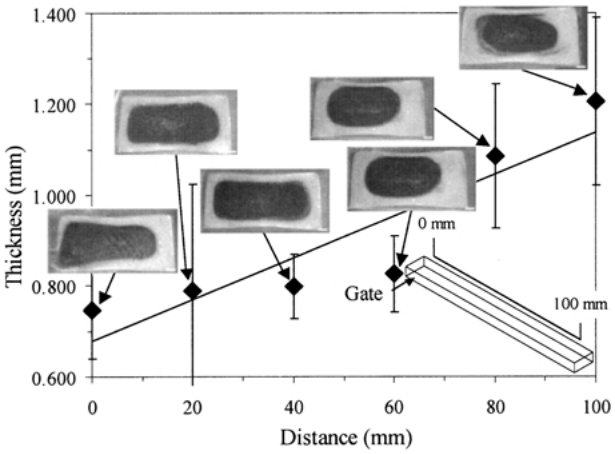

Figure 5 Variation of the average outer layer thickness along the flow path for the impact test bars together with the cross-section micrographs at 0, 20, 40, 60 80 and 100 mm from the gate point (scale bar is 1 mm).

perpendicular to the MDF. The reinforcing effect of the C fiber is limited to the former region.

The impact test curves for both bi-composite and HDPE/C fiber moldings are presented in Fig. 4, together with the respective values of F_p, U_p and U_b divided by the correspondent cross-section in order to account for the different molding dimensions employed for each case. The real values of the F_p, the U_p and the U_b can be readily obtained by multiplying the values presented for the bi-composite and the HDPE/C fiber composite moldings by $6 \times 13\,mm^2$ and $4 \times 10\,mm^2$, respectively. The bi-composite and the HDPE/C fiber composite moldings present identical values of force at peak (F_p of $13\,N/mm^2$). Nevertheless, the energy absorbed during the crack initiation is significantly lower for the sandwich moldings (U_p of $0.009\,J/mm^2$), probably as a result of the higher brittleness of the HDPE/HA surface layer as compared to the tougher HDPE/C fiber composite (U_p of $0.014\,J/mm^2$). In spite of this, the energy absorbed during the propagation stage for the bi-composite moldings (U_f of $0.018\,J/mm^2$) is higher than the obtained for the single HDPE/C fiber composites (U_f of $0.017\,J/mm^2$).

Fig. 5 presents the evolution of the average outer layer thickness along the flow path for the impact bars together with the respective cross section micrographs. At the vicinity of the gate point (0 mm), the skin is thin as a consequence of the high thermal level of this region during the filling stage, which originates an asymmetrical morphology. As the distance from the gate point increases, the sandwich morphology becomes more symmetric (20 and 40 mm). This increase in symmetry is associated with a thickening of the HDPE/HA outside layer. Nevertheless, such increase is not homogeneous along the cross section perimeter, being more pronounced near the edges of the molding. This effect can be minimized by a proper adjustment of the flow rate, since constant core dimensions are favored by low injection speeds [19, 20]. For this molding geometry, the penetration of the skin by the core material is less pronounced than that observed for the tensile test specimens. The different thermal levels employed for the two compounds explain the higher definition of the sandwich morphology developed for this molding geometry. In fact, the respective molding set-up was based on an average barrel temperature of the horizontal unit (that contains the core material) 50 °C lower, on average, than the vertical unit (that contains the skin material), as shown in Table I. This set-up favored a high viscosity ratio and the even core distribution here observed.

Fig. 6 presents the SEM photographs of the impact fracture surfaces of the bi-composite moldings. The sandwich-like morphology delaminates upon the impact testing as it can be seen in Fig. 6(a), creating an interface between the HDPE/C fiber and the HDPE/HA composites. This phenomenon occurs in the transition region between the two materials. Fig. 6(b) presents the detailed view of the transition region signalled in Fig. 6(a), where it is possible to observe the presence of both the C fiber and the HA particles. In this region (600 μm in length approximately), the HDPE matrix alters considerably its mechanical behavior. The ductile fracture surface on the upper left (UL) part of the figure, associated to the presence of the C fiber, gives place, on the lower right (LR) part of the figure, to a brittle fracture surface, in which C fiber and HA particles coexist. Following further the UL → LR direction in Fig. 6(b), it reached the interface created by detachment of the outer surface layer upon the impact testing. This interface defines the line from which interpenetration of the skin by the core starts to occur. The detached HDPE/HA layer, presented in Fig. 6(c), does not contain any C fiber.

3.2. Bioactivity testing results

Figs. 7 and 8 present respectively the SEM photographs of the surface of unpolished and polished samples after 0 ((a) in Figs. 7 and 8), 7 ((b) and (c) in Figs. 7 and 8) and 30 ((d) and (e) in Figs. 7 and 8) days of immersion in SBF. In Figs. 7(a) and 8(a) it is possible to observe the surface of the unpolished and polished specimens before their respective immersion in SBF. The dispersion of the HA particles in the polymer matrix is high for the two cases. However, it is evident the higher surface roughness and the higher number of HA particles at the surface of the polished samples, as a result of the removal of the deep frozen layer with very low HA content. The removal of this layer is expected to benefit the bioactive behavior of the molding, since it increases the HA

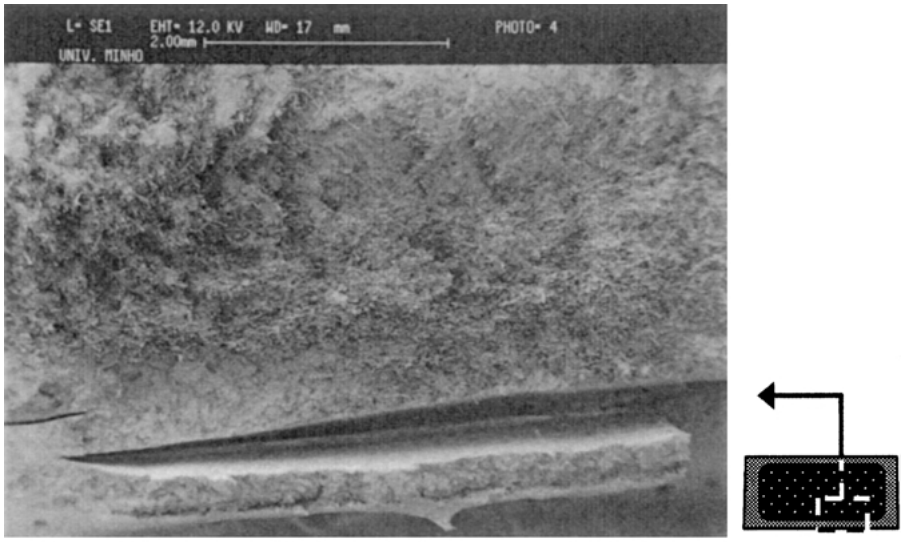

(a)

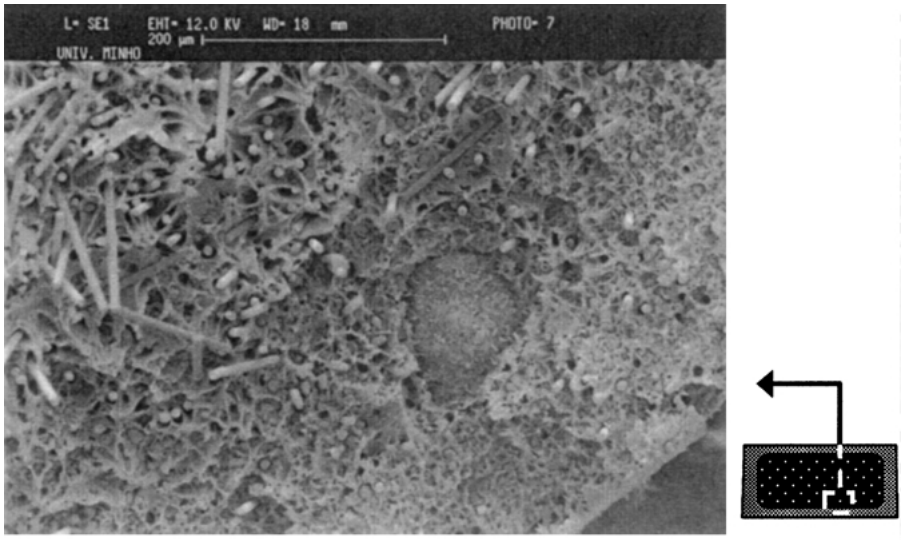

(b)

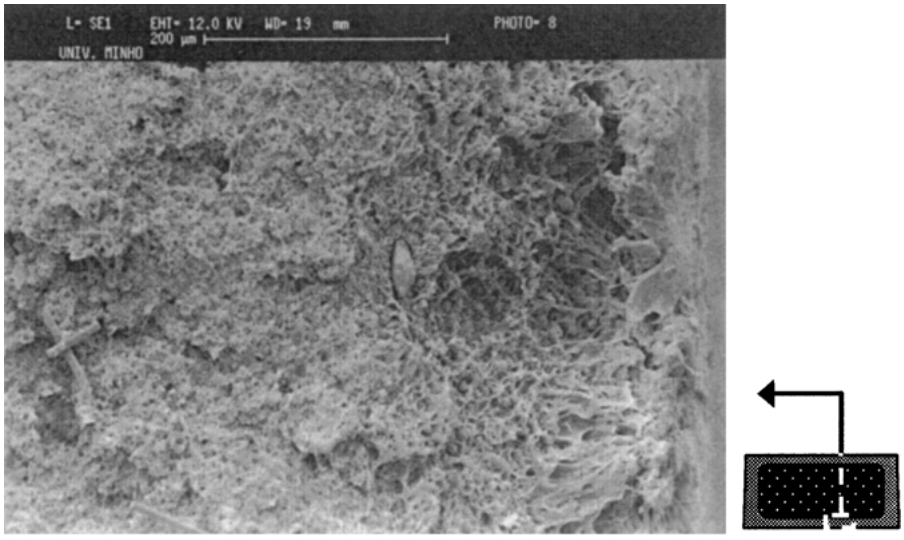

(c)

Figure 6 Scanning electron microscope photographs of the fracture surface of the bi-composite moldings after impact testing: (a) general view, (b) detailed view of the transition region between the HDPE/HA outer layer and the HDPE/C fiber core and (c) detailed view of the HDPE/HA outer layer.

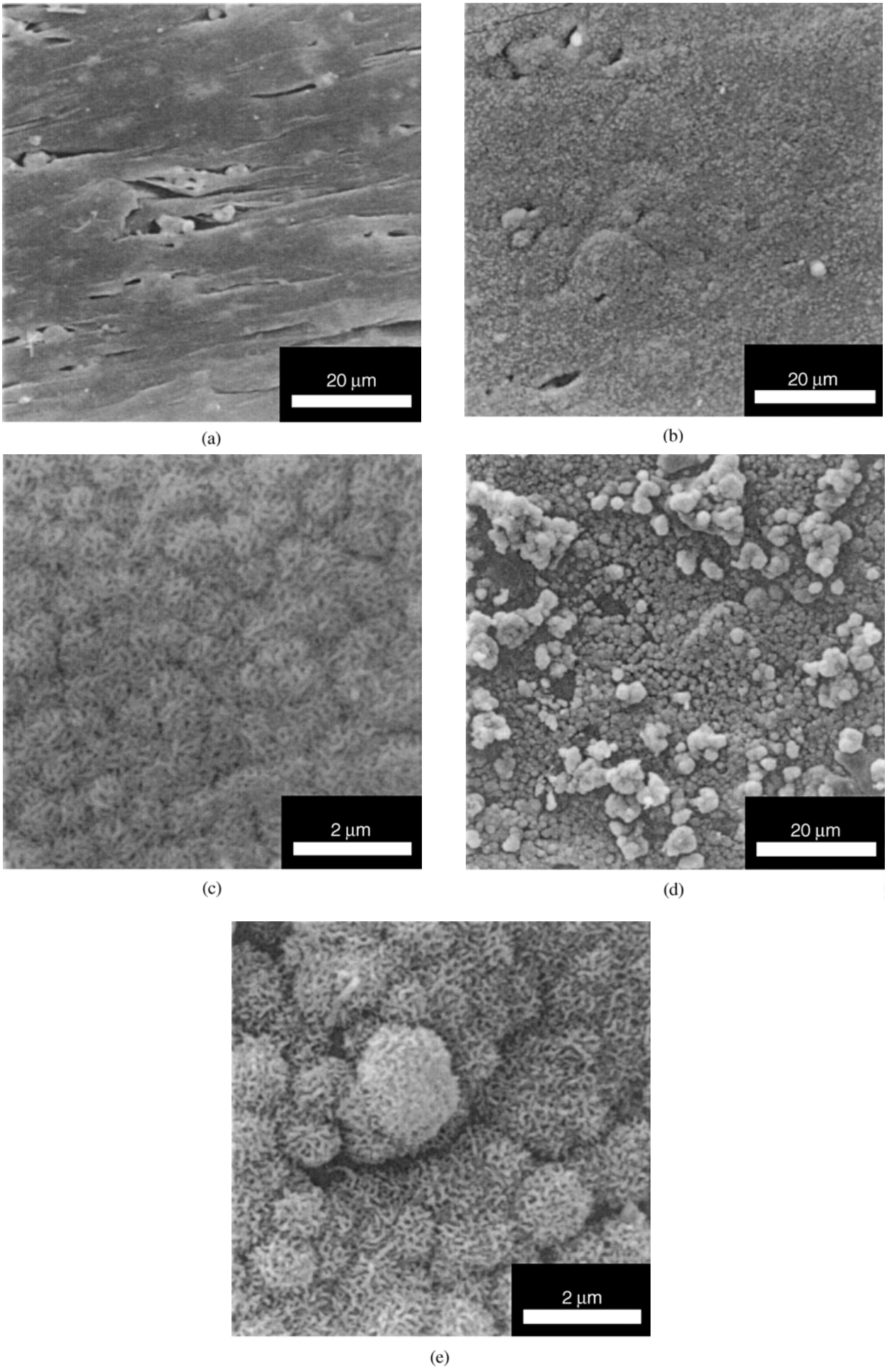

Figure 7 Scanning electron microscope photographs of the surface of unpolished bi-composite specimens after (a) 0, (b) and (c) 7 and (d) and (e) 30 days of immersion in SBF.

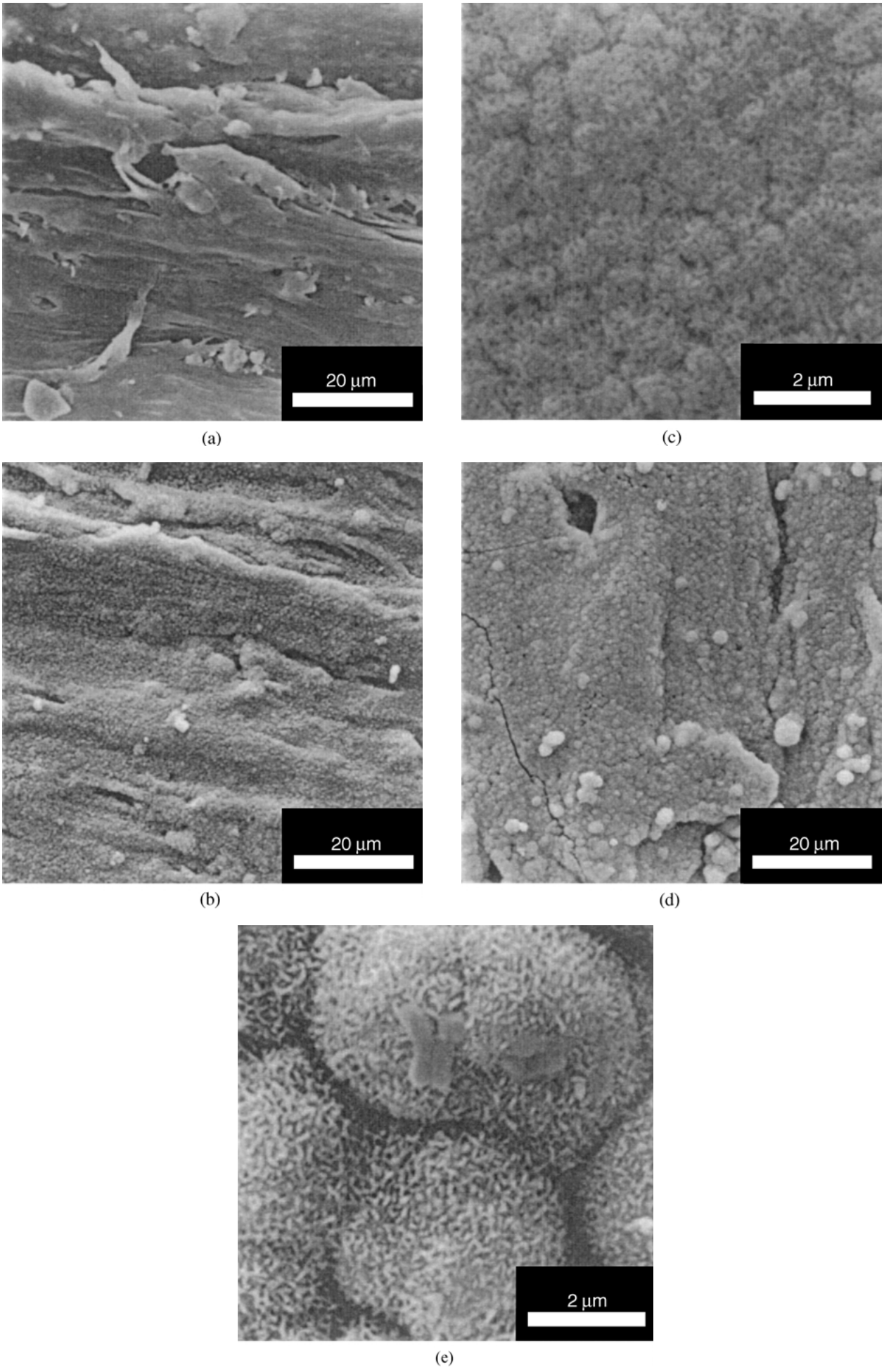

Figure 8 Scanning electron microscope photographs of the surface of polished bi-composite specimens after (a) 0, (b) and (c) 7 and (d) and (e) 30 days of immersion in SBF.

volume content at the composite surface. As previously shown by the work of Bonfield and his co-workers, a bioactive behavior will occur beyond a minimum volume content of HA of about 20% [21]. Above this minimum, the HA particles in the surface act as nucleation sites for the formation of an apatite layer. For the HA content employed in this study (about 23% in volume) it is expected that the HDPE/HA surface layer presents a bioactive character, in accordance with the previous study carried out by our research group [22].

After 3 days of SBF immersion it is already possible to observe, at high magnifications (not presented here), the formation of the first small nuclei at the surface, particularly for the case of the polished specimens. This result suggests that the increase in the surface roughness is leading to a faster production of the first apatite nuclei during the first days of immersion. Some authors claim that the effect of roughness is related to the mechanical interlocking of the apatite layer to the substrate, that favors the film formation and its respective adhesion [23, 24]. Furthermore, upon the surface polishing, more HA particles become available, which increases the amount of nucleation sites for the apatite growth. After 7 days the formed nuclei have grown into a well-defined apatite-like layer that can be observed, for either the unpolished (Figs. 7(b) and (c)) or the polished (Figs. 8(b) and (c)) samples. In both cases, the formed layers appear extremely compact when observed at low magnifications. Nevertheless, at higher magnifications, a finer structure is observed formed by agglomerated needle-like crystals, giving rise to the so-called cauliflower morphology [24]. Figs. 7(d) and (e); and Figs. 8(d) and (e) show the morphology of the very cohesive apatite layers after 30 days of SBF immersion, that is more evident for the polished samples (Figs. 8(d) and (e)). In this case the apatite layer seems thicker and more adherent, as it should be expected. Although not shown, it was not possible to detect any bioactive behavior for the HDPE used as a control.

Fig. 9 shows the EDS spectra for unpolished (Fig. 9(a)) and polished (Fig. 9(b)) materials, before and after SBF immersion. The intensity of the peaks, corresponding to the presence of Ca and P elements at the surface of the materials, seems to increase with time of immersion in SBF, while the peaks corresponding to the polymer phase decrease. It should be stated herein that appropriate routines for precise semi-quantitative EDS analysis have been used. Taking this into account, it might be said that this result can be regarded as an indication of the growing of a surface layer along immersion time as observed on the SEM micrographs.

Fig. 10 presents the Ca/P and $(Ca + Mg + Na + K)/P$ ratios calculated for the growing apatite layers for periods of immersion up to 30 days. EDS analysis of the formed films shows Ca/P ratios in the 1.5–1.7 range, i.e. between tricalcium phosphate (TCP) and HA (Fig. 10(a)). The values calculated for the $(Ca + Mg + Na + K)/P$ ratio are higher than for the Ca/P ratio, indicating that the presence of Na, Mg and K in the structure of HA (Fig. 10(b)) should be considered.

Fig. 11 shows the thin-film X-ray diffraction spectra of the surfaces before and after different periods of SBF immersion. The peaks on these figures corresponds to the

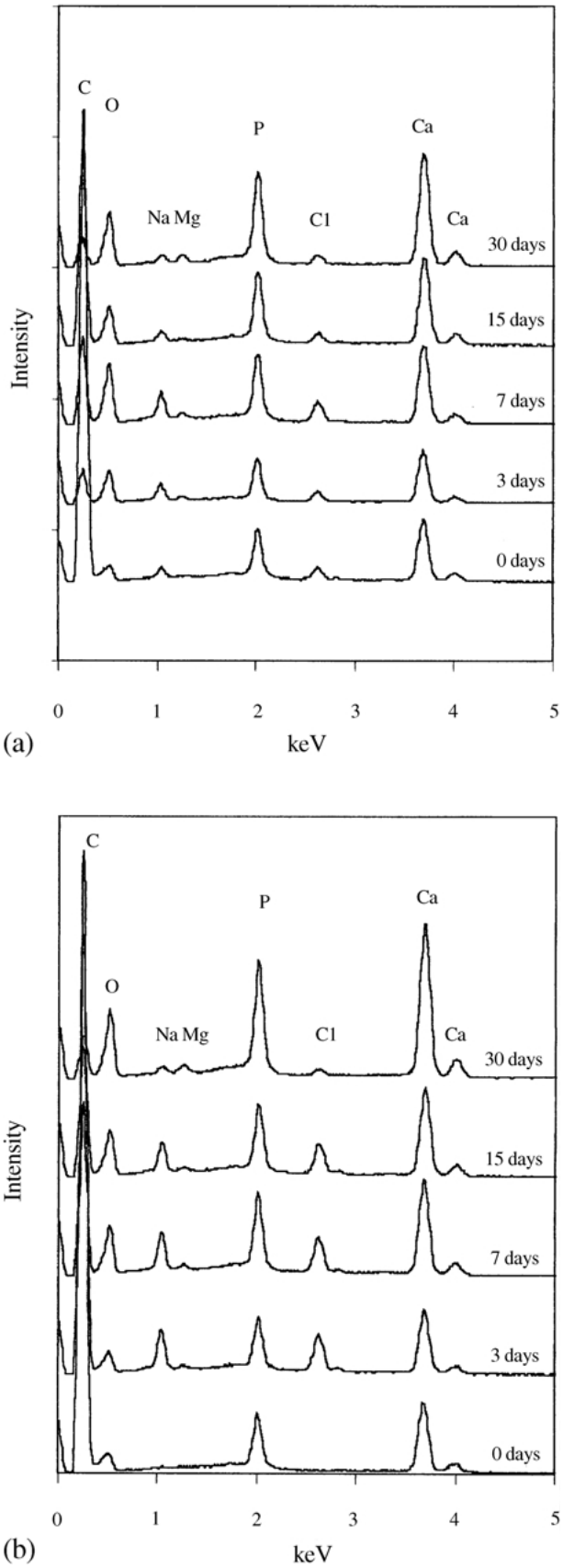

Figure 9 Energy dispersive spectroscopy spectra of (a) the unpolished and (b) the polished HDPE/HA substrates before and after immersion in SBF for periods up to 30 days.

main characteristic of HA (standard spectra, JCPDS 9-432) and PE. For 0 days, the crystalline peaks observed correspond to the PE matrix and the synthetic HA used as a filler in the composite. In accordance with the EDS results, the intensity of the peaks assigned to HA, for the

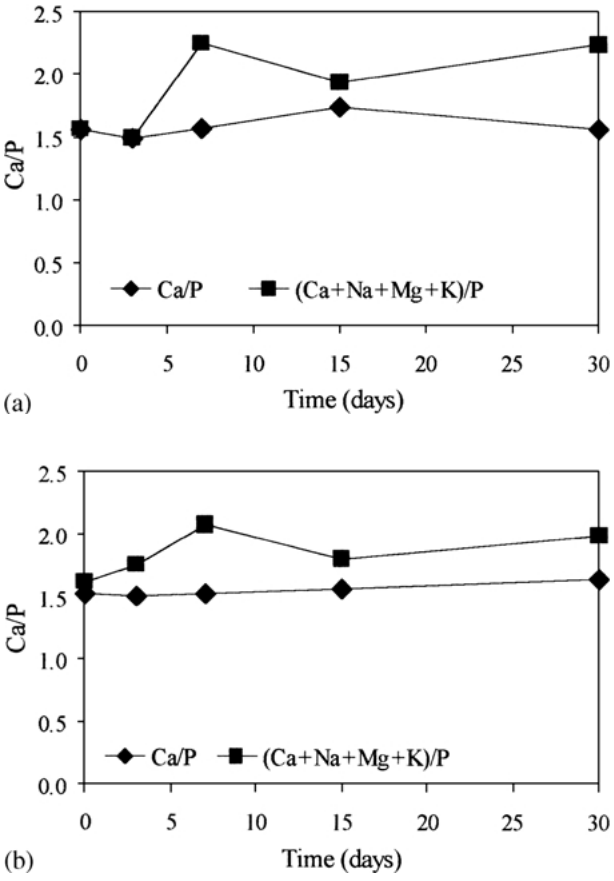

Figure 10 Evolution of the Ca/P and (Ca + Mg + Na + K)/P ratios as a function of the immersion period in SBF of the apatites formed on (a) the unpolished and (b) the polished HDPE/HA substrates.

case of the polished samples, is higher, which indicates that a higher HA concentration is available at the surface. Upon SBF immersion, the intensity of the PE peaks decrease gradually with period of immersion, indicating that a layer is growing and gradually covering the surface of the composite. HA peaks also decrease with the immersion time, which indicates that a partially amorphous Ca–P layer is forming, similar to human bone apatite.

In Fig. 12 the evolution of Ca and P elemental concentrations (obtained by ICP spectroscopy) in the SBF solution is plotted as a function of the immersion time. Ca and P concentrations decrease in the solution, suggesting that precipitation of Ca and P is taking place, leading to the formation and growth of a Ca–P layer, as observed by SEM, EDS and TF-XRD. This decrease is more evident in the first 7 days of immersion (known as the induction period), when the apatite nuclei are growing in order to form a continuous layer, consuming, during such period, higher amounts of Ca and P. When comparing the evolution of the solutions for unpolished (Fig. 12(a)) and polished (Fig. 12(b)) materials, it is possible to observe that for the polished specimens there is a greater decrease in the concentrations of Ca and P demonstrating that a thicker layer is growing in the surfaces with higher roughness. This result is in agreement with the SEM micrographs and EDS spectra previously presented.

Table III presents the pH values of the solutions for the different times of immersion in SBF. After 3 days, the pH

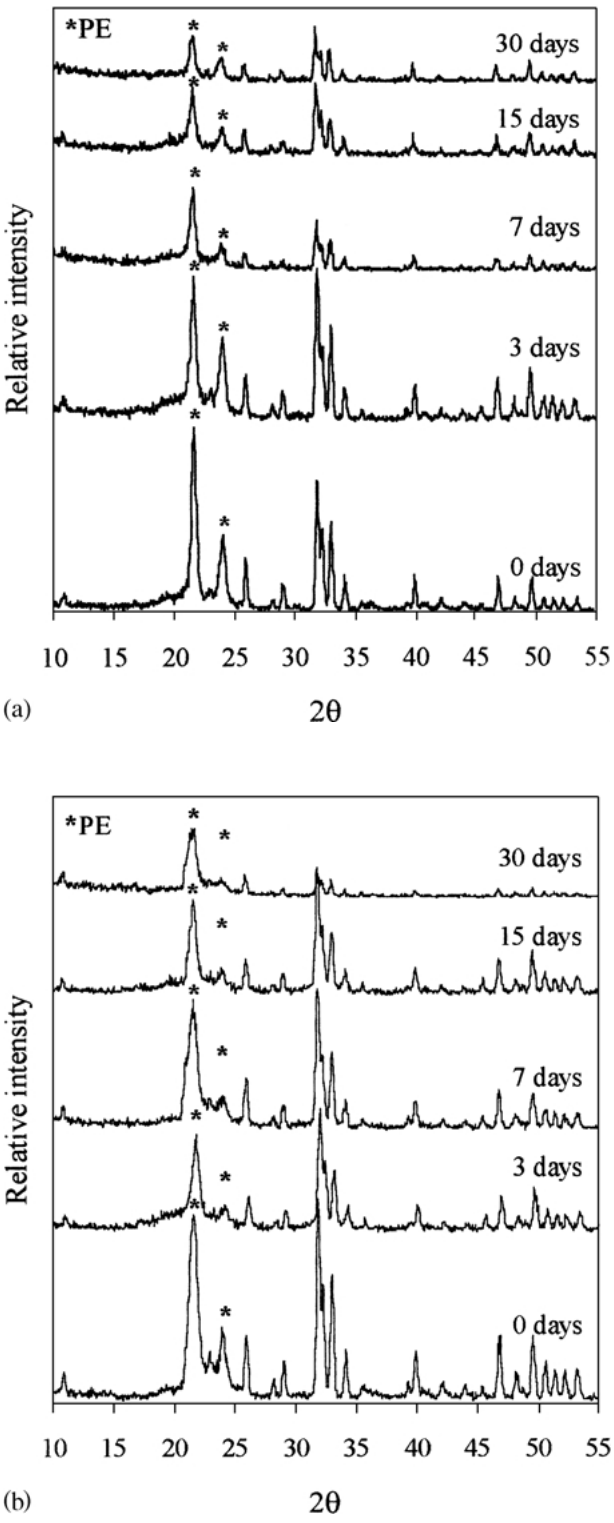

Figure 11 Thin film X-ray diffraction patterns of the film formed on (a) the unpolished and (b) the polished substrates after 0, 3, 7, 15 and 30 days of immersion in SBF.

TABLE III pH of the SBF solution after different immersion times

Time (days)	pH (Unpolished)	pH (Polished)
0	7.40 ± 0.04	7.40 ± 0.04
3	8.48 ± 0.08	8.67 ± 0.15
7	8.36 ± 0.17	7.74 ± 0.07
15	8.22 ± 0.09	8.60 ± 0.13
30	8.25 ± 0.05	8.58 ± 0.16

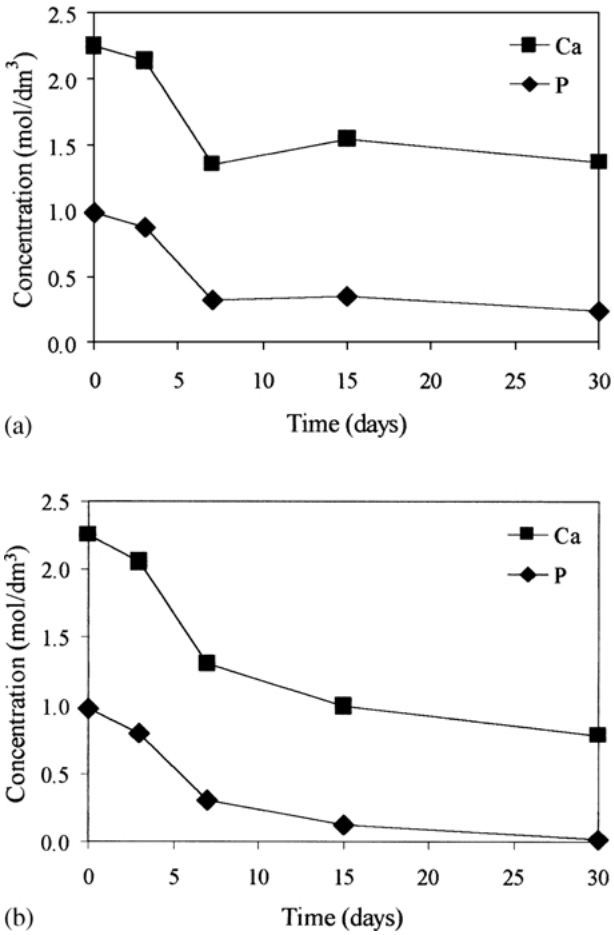

Figure 12 Evolution of the Ca and P elemental concentration in the solution as a function of the immersion time in SBF solution for (a) the unpolished and (b) the polished bi-composite moldings as determined by induced coupled plasma emission (ICP) spectroscopy.

of the solutions rises from 7.40 to 8.48 and 8.67 for respectively the unpolished and the polished samples. This increase is probably due to some dissolution of the filler (HA), which leads to an increase in Ca and P concentration. ICP results show that after 3 days the decrease in Ca and P is not so accentuated as it would be expected. These results suggest that a balance between the dissolution of the filler (that causes increase of Ca and P concentration) and precipitation of a Ca–P layer in the surface (that causes a decrease of Ca and P concentration) occurs. For longer periods of SBF immersion, the pH is not expected to change.

4. Conclusions

Composites featuring a sandwich-like morphology were successfully produced by injection molding. These moldings comprise a HA filled HDPE surface layer and C fiber reinforced core. The research approach based on the selective C fiber reinforcement of the molding core was shown to be a valid route for the enhancement of stiffness of HDPE/HA composites. Upon mechanical testing, the bi-composite sandwich moldings exhibits two distinct modes of fracture: a relatively brittle fracture associated to the HA filled surface layer and more ductile fracture mode related to C fiber reinforced molding core. The inferior mechanical performance of the bi-composite moldings, as compared with the HDPE/C fiber composites, is related to the brittle character, the high thickness and the uneven distribution of the HDPE/HA surface layer.

As a result of the HA loading, the sandwich bi-composite moldings exhibit a clear *in vitro* bioactive behavior under simulated physiological conditions, which indicates that an *in vivo* bone-bonding behavior can be eventually expected for these materials. The mechanical removal of the frozen layer in the bi-composite moldings enhances considerably the bioactive character of these moldings since it increases the HA volume content at the surface.

The control of the morphological development of the bi-composite materials by means of the optimization of the molding operating conditions, together with the use of suitable composite formulations is expected to lead to the successful development of bone-analog composites featuring simultaneously a bone-matching mechanical performance and a clear bioactive behavior.

Acknowledgments

The authors want to acknowledge the help of Dimitre Tchalamov during injection molding. Rui A. Sousa also acknowledges the support of Subprograma Ciência e Tecnologia do 2° Quadro Comunitário de Apoio, Ministério da Ciência e Tecnologia (Portugal).

References

1. W. BONFIELD, M. D. GRYNPAS, A. E. TULLY, J. BOWMAN and J. ABRAM, *Biomaterials* **2** (1981) 185.
2. R. B. MARTIN and D. B. BURR, ''Structure, Function and Adaptation of Compact Bone'' (Raven, New York, 1989).
3. A. RAVAGLIOLI, A. KRAWJEWSKI, G. C. CELLOTI, A. PIANCASTELLI, B. BACHINNI, L. MONTANARI, G. ZAMA and L. PIOMBI, *Biomaterials*, **17** (1996) 617.
4. G. P. EVANS, J. C. BEHIRI, J. D. CURREY and W. BONFIELD, *J. Mater. Sci: Mater. Med.* **1** (1990) 38.
5. S. A. GOLDSTEIN, *J. Biomech.* **20** (1987) 1055.
6. D. R. CARTER and W. C. HAYES, *Clin. Orthop.* **135** (1978) 192.
7. V. ZIV, H. WAGNER and S. WEINER, *Bone* **18** (1996) 417.
8. S. WEINER, T. ARAD, I. SABANAY and W. TRAUB, *Bone* **20** (1997) 509.
9. K. HATA and T. KOKUBO, *J. Am. Soc.* **78** (1995) 1049.
10. W. BONFIELD, in ''Monitoring of Orthopaedic Implants'', edited by F. Burny and R. Pruers (Elsevier Science Publishers, Amsterdam, 1993).
11. W. BONFIELD, *J. Biomech.* **20** (1987) 1071.
12. R. A. SOUSA, R. L. REIS, A. M. CUNHA and M. J. BEVIS, *J. Appli. Polym. Sci.* **86** (2002) 2873.
13. A. L. OLIVEIRA, C. ELVIRA, R. L. REIS, B. VÁZQUEZ and J. SAN ROMÁN, *J. Mater. Sci. Mater. Med.* **10** (1999) 827.
14. G. KALAY, R. A. SOUSA, R. L. REIS, A. M. CUNHA and M. J. BEVIS, *J. Appl. Polym. Sci.* **73** (1999) 2473.
15. R. L. REIS, A. M. CUNHA, M. J. OLIVEIRA, A. R. CAMPOS and M. J. BEVIS, *Mat. Res. Innovat.* **4** (2001) 263.
16. R. A. SOUSA, R. L. REIS, A. M. CUNHA and M. J. BEVIS, *Plas. Rubb. Comp.* submitted.
17. C. JAROSCHEK, R. STEGER, W. NESCH, A. GEHRING and K. BOURDON, U.S. Patent 5,443,378 (1995).
18. D. J. LEE, A. I. ISAYEV and J. L. WHITE, *SPE Technical Papers* **44** (1998) 346.
19. R. SELDÉN, *Polym. Eng. Sci.* **40** (2000) 1165.
20. K. KUHMANN and G. W. EHRENSTEIN, SPE Annual Technical Conference (1998).
21. W. BONFIELD, in Bioceramics 11, edited by R. Z. Legeros and J. P. Legeros (World Scientific, Singapore, 1998), p. 37.

22. R. L. REIS, A. M. CUNHA and M. J. BEVIS, in Bioceramics 10, edited by L. Sedel and C. Rey (Paris, France, Out., Elsevier Science, Amsterdam, 1997) p. 515.
23. M. TANAHASHI, T. YAO, T. KOKUBO, M. MINODA, T. MIYAMOTO, T. NAKAMURA and T. YAMAMURO, *J. Amer. Ceram. Soc.* **77** (1994) 2805.
24. R. L. REIS, A. M. CUNHA, M. H. FERNANDES and R. N. CORREIA, *J. Mater. Sci. Mater. Med.* **8** (1997) 897.

Received 25 June
and accepted 20 August 2002